Recuperating Advanced Propulsion Engine Redesign

Andrew Marshall*, Kevin Bieri*, David Bright*,
Kevin Gomez*, Kevin Horn*, Becca Lidvall*,
Carolyn Mason*, Peter Merrick*, Jacob Nickless*
University of Colorado, Boulder CO, USA

Miniature turbojet engines present a number of advantages over traditional propeller-driven propulsion systems for small Unmanned Air Vehicles (UAVs); however, increased fuel consumption for turbojets has delayed their adoption. The purpose of the REcuperating Advanced Propulsion Engine Redesign (REAPER) project is to model, build, implement, and verify a recuperative system integrated into an existing JetCat P90-RXi miniature turbojet engine to decrease thrust specific fuel consumption while preserving the engine's thrust. Analysis of the engine was conducted using a control volume model which incorporated empirical models and conservation laws to predict the evolution of the flow variables through the engine. The REAPER recuperator was designed via a series parametric studies conducted on the model. These studies revealed that in order to maximize the decrease in thrust specific fuel consumption for the P90-RXi, minimizing pressure losses is paramount when maximizing heat transfer.

Nomenclature

A	=	Area
C_f	=	Skin Friction Coefficient
D_h	=	Characteristic Length
h	=	Convective Heat Transfer Coefficient
HV	=	Heating Value
k	=	Thermal Conductivity
$\dot{m}_f$	=	Mass Flow Rate of Fuel
Nu	=	Nusselt Number
Pr	=	Prandlt Number
$\dot{Q}_{combustion}$	=	Rate of Heat Addition During Combustion
$\dot{Q}_x$	=	Rate of Heat Addition due to Heat Transfer
Re	=	Reynolds Number
T_o	=	Total Temperature
t	=	Thickness
U	=	Heat Transfer Coefficient
$\dot{W}_{shaft}$	=	Rate of Shaft Work Production
η_b	=	Burner Efficiency
δ	=	Fin Thickness
p	=	Pressure
ρ	=	Density
V	=	Bulk Velocity
T	=	Bulk Temperature
C_p	=	Specific Heat
F_{fric}	=	Force due to Friction
η_0	=	Heat Transfer Area Effectiveness
η_f	=	Heat Transfer Fin Effectiveness

*University of Colorado at Boulder, Aerospace Engineering Sciences Undergraduate Student

I. Introduction

The REAPER recuperative system will provide increased fuel efficiency for the JetCat P90-RXi when compared to its stock engine performance. The JetCat P90-RXi is a miniature turbojet engine that is typically used in small unmanned air vehicles (UAV). UAV's have broad mission applications within both military and civilian markets. With ever increasing demand for expanded UAV flight regimes, more powerful and efficient engines are required. Traditionally, small UAV's have exclusively utilized electric or piston propeller propulsion systems due to the high efficiency and low specific fuel consumption. Comparatively, turbojets allow UAV's to fly at higher altitudes and airspeeds; however, miniature turbojets inherently have a higher specific fuel consumption. To expand the flight envelope while maintaining high efficiency, the miniature turbojet must be improved.

A common device to increase engine efficiency is a recuperator. A recuperator is a heat exchanger that recovers waste heat from the engine exhaust to be reintroduced into the cycle prior to combustion in order to reduce the amount of fuel burn necessary to reach the same turbine outlet temperature. Recuperator for turbine engines have traditionally been applied to large ground-based electrical power generation systems. These engines are extremely efficient; however, they are also extremely heavy. A successfully recuperating turbojet engine would provide decreased specific fuel consumption while maintaining the benefits of turbojet propulsion. The research and development provided by project REAPER will test the feasibility for future development of a flight ready recuperating turbojet engine, which would increase range and altitude performance for small UAV's, expanding mission capabilities for military and civilian applications alike.

II. Design Objectives

The REAPER project is sponsored by the Air Force Research Labs (AFRL) to research jet engine recuperation technology. AFRL provided five goals to the team: (*1*) Design/build a device to recuperate heat on a JetCat P90-RXi engine, (*2*) Quantify changes in thrust specific fuel consumption, (*3*) Preserve as much stock engine thrust as possible, (*4*) Analyze/characterize any changes in engine thrust and throttle response, (*5*) Minimize weight and volume addition.

Considering these requests, the REAPER teams developed three main objectives for the project: design and manufacture a recuperator system, integrate the recuperator on the engine, and run the engine in the modified configuration. In order to design the recuperator, a high fidelity model is necessary to predict the thrust and fuel consumption change with recuperation. Therefore, the three levels of success are defined with respect to the model/simulation and the engine recuperator hardware milestones as shown in Table 1. The levels of success characterize whether the project goals were achieved.

Success Level	Project Description	
	Simulation	Recuperator/Engine
Level 1	• First order, one-dimensional, steady state engine thermal modeled with recuperator design integrated meets recuperator thrust specific fuel consumption reduction (10%), and thrust reduction (10%) requirements	• Recuperator designed and manufactured • Recuperator tested with engine analog at dimensionally scaled steady-state, full-throttle operating conditions
Level 2	• Thermal model includes transient performance	• Recuperator integrated into P90-RXi engine • Engine starts and runs at at full throttle for 120 seconds with the integrated recuperator
Level 3	• CFD model of the recuperator developed with effectiveness matching actual recuperator test data within 25%	• Engine with integrated recuperator runs continuously for full throttle range • Engine runs at full throttle with recuperator integrated, for at least 4 minutes • Engine throttle time from 50% to 100% is within 100% of stock throttle

Table 1. REAPER Levels of Success

The design requirements addressed in Table 1 were derived from the three main functional requirements of the project:

1. The thrust specific fuel consumption (TSFC) of the engine with the heat exchanger system integrated shall decrease by at least 10% at maximum thrust.

2. The simulation shall model the thrust and efficiency of the engine with the integrated heat exchanger system.

3. The engine electronics shall operate the JetCat P90-RXi engine with integrated recuperator.

These functional requirements were developed from the sponsor requests, and translate directly into the critical project elements: the heat exchanger, modeling, electronics, and testing. The first functional requirement was derived from research about existing recuperators. The heat exchanger is the critical component that transfers heat effectively while keeping cost, manufacturability, and integration in mind. To characterize the recuperator effectiveness as well as the change in TSFC of the engine, sensor choice and location as well as the test procedures are a key component of project REAPER. The second functional requirement is needed in order to drive the design of the recuperator and predict its results. The second critical project element is therefore the thermal-fluid modeling, which characterizes the system and allows for better design methods and validation through testing. Finally, the last functional requirement addresses the need for custom REAPER electronics to run the engine in the modified configuration. As the stock electronics are a "black box" that do not allow modification and the recuperator changes the fuel characteristics of the running engine, they are not a viable option for use in running the modified engine. The progress on each critical project element drives the allocation of time and resources during both the design methodology and results phases of the project.

III. Design Methodology

A. Preliminary Analysis

As discussed by Kays and London[12], the primary trade-off in the design of a heat exchanger is the balance of pressure losses to heat transfer inside the heat exchanger. In the case of the REAPER design; however, the importance of minimizing pressure losses was even higher than normal. Figure 1 gives the results of an extremely simplified model of the thrust specific fuel consumption of the engine versus the heat transfer provided by the recuperator and the pressure losses on either side of the recuperator. Each contour represents a 2000 Pa increase in the pressure loss on the cold side of the heat exchanger. The model showed that at the scale of the REAPER recuperator which preliminary analysis estimated to have an overall heat transfer rate of less than 2000 W, would need to have extremely low pressure losses (order of $2 * 10^3$) in order to have any net benefit to the thrust specific fuel consumption of the engine. As a result, rather than attempting to maximize the heat transfer coefficient for the REAPER recuperator, the design would attempt to minimize pressure losses with the higher heat transfer rates being a secondary goal.

B. Detailed Design

Detailed design of the REAPER recuperator was primarily conducted through a series of parametric studies on a control volume model of the engine. Once the parametric study returned a design, the results of the control volume model were verified using a computational fluid dynamics (CFD) model of the recuperator in SolidWorks Flow Simulation.

1. Control Volume Model

Control volume analysis is a first order flow analysis method which divides the engine into a series of control volumes then uses simplified conservation laws and empirical correlations to predict the change in flow variables between the entrance and exit of each control volume. Additionally, due to the complexity of modeling the performance of the turbo machinery and combustion chamber of the engine, empirically derived component efficiencies were employed in the control volume code. The flow variables tracked in the control volume model are the bulk average velocity, density, pressure, and temperature of the fluid. Figure 2 shows a general flow diagram for the control volume model.

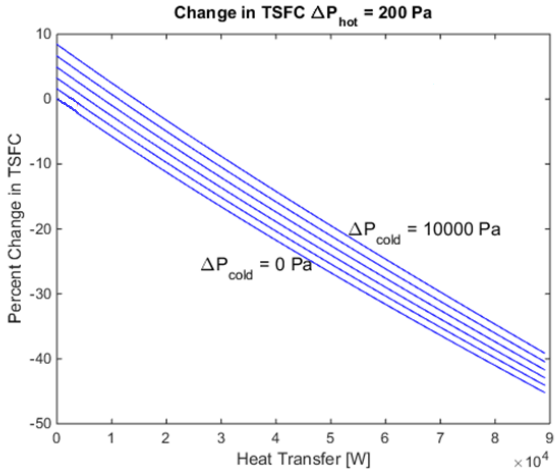

Figure 1. Thrust Specific Fuel Consumption verse Heat Transfer with Pressure Loss Curves.

The basis for the control volume are conservation laws for mass, momentum, and energy as well as a constitutive law to completely characterize the thermodynamic state of the flow variables. Equations 1 to 4 give the conservation equations for mass, momentum, and energy as well as the constitutive ideal gas law equation for each control volume.

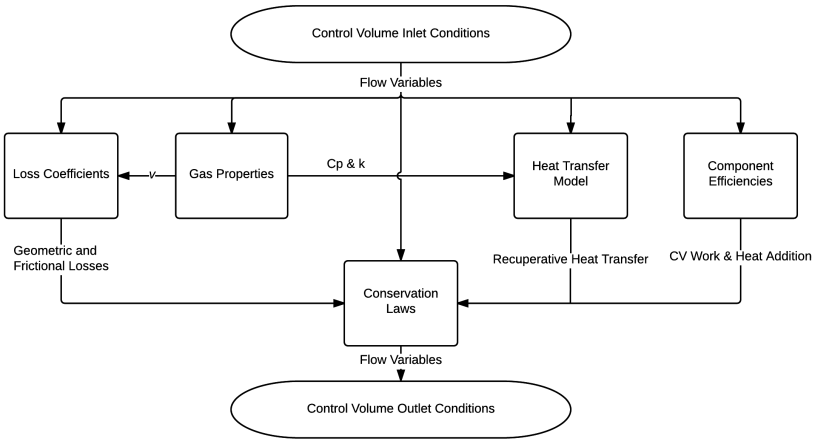

Figure 2. Control Volume Model Flow Diagram.

Conservation of mass:

$$\rho_1 A_1 V_1 = \rho_2 A_2 V_2 \qquad (1)$$

Conservation of momentum:

$$p_1 A_1 - p_2 A_2 - \left(\frac{\dot{W}_{shaft}}{V_m} - F_{fric} \right) = \dot{m}_2 V_2 - \dot{m}_1 V_1 \qquad (2)$$

Conservation of energy:

$$\frac{\dot{Q} - \dot{W}_{shaft}}{\dot{m}} - \frac{1}{2} {V_m}^2 K_L = C_{p,m} (T_2 - T_1) + \frac{1}{2} \left({V_2}^2 - {V_1}^2 \right) \qquad (3)$$

Ideal gas law:

$$P = \rho R T \qquad (4)$$

In Eqs. 1 to 4, a subscript 1 implies the entrance of a control volume, a subscript 2 implies the exit of control volume, and a subscript m implies a weighted average of the two values in manner recommended by Miller (taken as 60% of the initial value and 40% of the final value).[27] In Eq. 2 F_{fric} is the force due to wall friction acting on the fluid and is given by Eq. 5, where C_f is skin friction coefficient from the Colebrook-White formula and A_w is the total wall area of the control volume.[23]

$$F_{fric} = \frac{1}{2} \rho_m {V_m}^2 C_f A_w \qquad (5)$$

In Eq. 3, K_L is the overall loss coefficient due frictional and geometric effects in the control volume. All the loss coefficients are specific pressure losses resulting from the unrecoverable losses due to turbulent and viscous dissipation in the control volume. Miller details the calculation of the coefficients which include pressure loss sources such as sudden expansion or compression, separation in diffusers and flow diversion (i.e. turning the flow).[27]

In Eqs. 2 and 3, $\dot{Q}$ and $\dot{W}_{shaft}$ are the rate of heat addition and rate of shaft work production for the control volume. Heat transfer effects inside the engine result from two main sources, convective heat transfer or combustion. In the case of combustion, the heat transfer is calculated using Eq. 6 where η_b is the burner efficiency (taken as 0.946) and HV is the lower heating value of the fuel (~46.2 MJ for kerosene).

$$\dot{Q}_{combustion} = \eta_b \dot{m}_f HV \qquad (6)$$

Shaft work is only present in the compressor and turbine control volumes; in both control volumes component efficiencies were used instead of calculating frictional losses. The component efficiencies as well as the pressure change across the components are calculated from compressor and turbine maps generated by a previous CU aerospace senior project team.

Heat transfer effects were only considered in the two control volumes directly around the heat exchanger. In the heat exchanger control volumes, the Gnielinski correlation given by Eq. 7 is used to calculate the convective heat transfer rates. The Gnielinski correlation is a commonly used model for for predicting the Nusselt number for internal

flows. The Nusselt number, given by Eq. 8, is a non-dimensional quantity which characterizes the heat transfer rate at a solid boundary of a fluid where h is the convective heat transfer coefficient and k is the thermal conductivity of the fluid. In the Gnielinski correlation C_f is the skin friction coefficient, Re is the Reynolds number based on hydraulic diameter, and Pr is the Prandtl number given by Eq. 9 which describes the ratio between momentum and thermal diffusivity.

$$Nu = \frac{(C_f/2)(Re - 1000)Pr}{1 + 12.7\sqrt{C_f/2}(Pr^{2/3} - 1)} \tag{7}$$

$$Nu = \frac{hD_h}{k} \tag{8}$$

$$Pr = \frac{C_p\mu}{k} \tag{9}$$

By rearranging Eq. 8, the convective heat transfer coefficient for each side of the heat exchanger can be calculated. The overall heat transfer coefficient U in the heat exchanger normalized to the cold side area is given by Eq. 10. In Eq. 10 t_w is the wall thickness, k_w is the thermal conductivity of the wall, A_h is the surface area of the hot side of the heat exchanger, A_c is the surface area of the cold side of the heat exchanger, and η_0 is the area effectiveness given by Eq. 11. Equation 11 is a representation of the less effective heat transfer area added by fins A_f due to the fact any heat transferred must conduct through the fins. The effectiveness of a fins η_f is given by Eq. 12 where m is given by Eq. 13 in which l is the fin height, δ is the fin thickness, h is the local convection coefficient, and k is the thermal conductivity of the fin.

$$U = \frac{1}{\frac{1}{\eta_0 h_c} + \frac{A_c t_w}{k_w} + \frac{1}{\frac{A_h}{A_c} h_h}} \tag{10}$$

$$\eta_0 = 1 - \frac{A_f}{A}(1 - \eta_f) \tag{11}$$

$$\eta_f = \frac{tanh(ml)}{ml} \tag{12}$$

$$m = \sqrt{\frac{2h}{k\delta}} \tag{13}$$

2. *Control Volume Parametric Study*

Using the control volume model, three parametric studies on the length, hydraulic diameter, and fin effectiveness were conducted to determine the optimal recuperator geometry (measured by the largest predicted decrease in thrust specific fuel consumption). Due to the interdependency of the simulation variables, the parametric studies were conducted as a single Monte-Carlo simulation. Figures 3 and 4 show for the variation of the heat transfer rate and pressure drop across the heat exchanger normalized to the maximum value and taken at the cross-section containing the high decrease in thrust specific fuel. From the results, two conclusions are readily drawn. First, the heat transfer rate increases at a slower rate than the pressure loss with increasing heat exchanger length, indicating that a shorter heat exchanger will always have a high heat transfer to pressure loss ratio. Second, the hydraulic diameter has a clear optimum point at which the pressure loss is the lowest (represented by the thick vertical line in Fig. 4); however, reaching the point requires sacrificing approximately 17% of the heat transfer.

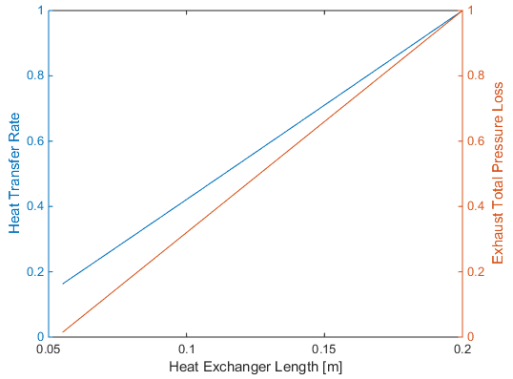

Figure 3. Normalized Change in Total Pressure and Heat Transfer Rate with Heat Exchanger Length.

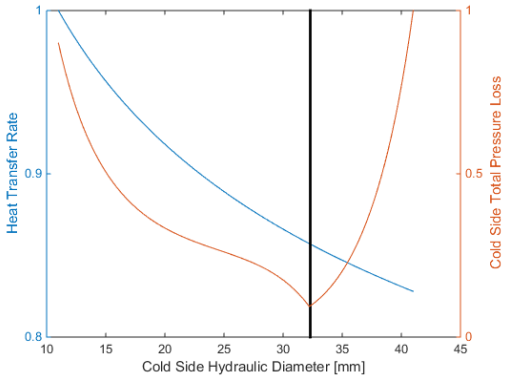

Figure 4. Normalized Change in Total Pressure and Heat Transfer Rate with Cold Side Hydraulic Diameter.

The third parametric study centered on varying the geometry of the heat exchanger fins to determine the effect on the fin effectiveness (a measure of how efficient fin surface area is compared to wall surface area). Figure 5 shows the variation in the change in thrust specific fuel consumption versus the number of fins on the cold side of the heat exchanger for the same cross-section of the design space containing the optimal solution. The plot reveals that the optimal number of fins is 13. However, due to a desire to maintain a fin number divisible by 4 to simplify later modeling as well as a desire to reduce fuel consumption by as much as possible to make measurements easier, 16 fins were ultimately selected for the design.

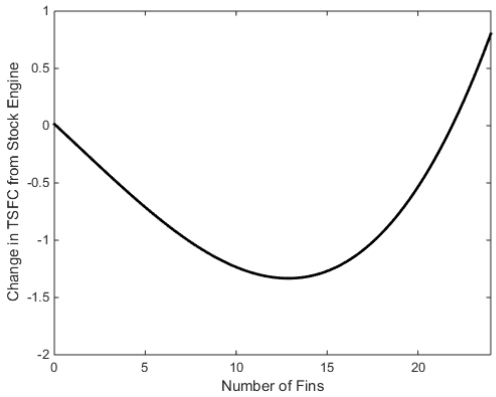

Figure 5. TSFC Change Verse Number Cold Side Fins.

3. SolidWorks Flow Simulation Model

Due to the low-order nature of the control volume model once the parametric study was completed, a higher order CFD model of the recuperator was created to verify the accuracy of the control volume model was high enough to trust the resulting design. To that end, a SolidWorks Flow Simulation model of just the heat exchanger was run. The simulation assumed specified mass flow rates for the entrance of the cold side of the heat exchanger Mesh independence was checked by running the simulation with 384k, 647k, and 1328k cells; the results of the CFD simulations as well as the control volume model are given in Table 2.

	Control Volume	CFD - 384K	CFD - 647k	CFD - 1328k
TSFC Reduction	1.18	1.20	1.20	1.20
Internal Pressure Drop [kPa]	1.52	1.48	1.48	1.48
External Pressure Drop [hPa]	1.87	2.10	2.00	2.60
Heat Transfer Rate [kW]	1.30	1.31	1.31	1.31

Table 2. Thermal-Fluid Model Results

IV. Design Results

A. Heat Exchanger Design

The analysis in the preceding sections indicated a combined heat exchanger/nozzle would be the most effective way to recover waste heat from the exhaust and reintroduce this heat into the engine's cycle. This meant that air coming from the compressor would need to be diverted to the back of the engine to pass over the heat exchanger nozzle before entering the combustion chamber. To maximize the amount of heat transferred between the exhaust and pre-combustion air, fins were to be added to the nozzle in order to increase the surface area available for heat transfer. Further analysis showed that thrust loss caused by external pressure losses (those on the exhaust side of the nozzle) would either completely nullify the improved thrust specific fuel consumption, or even reduce thrust enough to degrade the engine's fuel efficiency. As such, fins were only added to the internal (combustor) side of the heat exchanger. These decisions resulted in the finned heat exchanger nozzle shown in Fig. 6.

Due to the inherent complex geometry, REAPER outsourced the nozzle construction to ProtoLabs. This company created the nozzle with Direct Metal Laser Sintering (metal 3D printing) with titanium. Titanium was chosen because it had the best heat transfer coefficient for the lightest weight.

For this heat exchanger to be effective, six other groups of components were designed and manufactured to correctly route the air from the compressor, through the fins, and then into the combustion chamber. Ramped brackets were made to force the air outward to flow between the outer and inner casings, to the rear of the engine where end cap turns the flow back up toward the combustion chamber. From here, the air flows between the nozzle shroud and heat exchanger nozzle. This combination of components (shroud and nozzle) serves to create the exact areas demanded for heat transfer by the model. After passing through the heat exchanger, the air moves into the combustion chamber and is combusted as normal. These components can be seen integrated with the engine in Fig. 7.

Figure 6. Finned Heat Exchanger Nozzle.

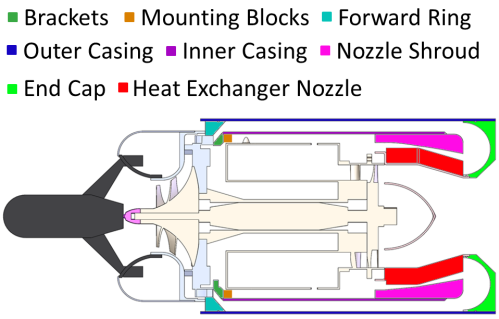

Figure 7. REAPER Components.

B. Verification and Validation

In order to verify and validate the results four major tests have been planned. These tests step through testing critical project elements including the recuperator, custom electronics, modified recuperator, and model. These tests directly correlate with REAPER's levels of success.

The first test is to make sure the heat exchanger can work in hot flow without critical failure and verify that the model is correct. The test setup is shown in Fig. 8, below. This test will satisfy level one success. In order to do this a test was set up with concentric pipe flow with heat exchanger for measured recuperation (T). Notice that the finned heat exchanger nozzle shown in Fig. 6 is in the center of the setup and performs as the recuperator. In order to reach the highest T for best measurement the hot flow was made as hot as possible without melting the test pipes. Two heat guns are used to generate the hot flow with a vacuum and a leaf blower for the cold flow. In order to match the model, each flow was set to have a turbulent Reynolds number (Re $>$10e4). An array of thermistors is used to measure the temperature profile in the cold flow in order to get the bulk average flow temperature. The thermistors have an error of 0.2C. Thermocouples are used to find a bulk temperature in the hot flow and have an error of 1.5C. Thermistors could not be used in the hot flow, because they cannot withstand expected hot temperatures of 300C. Velocity was measured with a pitot probe. The purple inserts in the flow depict flow straighteners which help to stop the flow from circulating the help produce repeatable results.

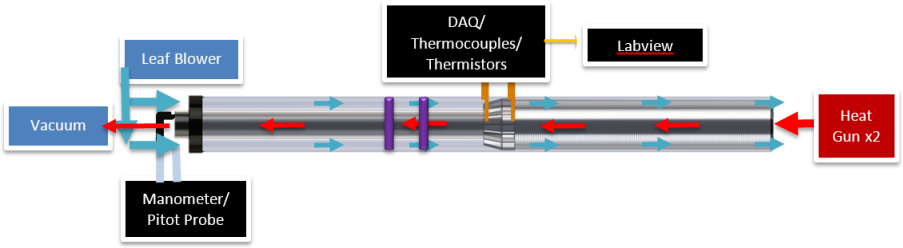

Figure 8. Concentric Pipe Flow with Heat Exchanger for Measured Recuperation (T).

Results from ten tests show the model matches the data within +5%. The plot, shown in Fig. 9, shows experimental data plotted in green and model results for the same conditions in blue. The error bars on the data are 0.4K, due to thermistor error. The error bars on the model points are two-sigma of the standard deviation of a Monte Carlo Simulation with 500 data points. The model is accurate since, the error bars on the experimental and model data overlap with each other. With this data, REAPER can trust that the model is accurate and can work the control volume model made for the modified engine.

The second and third test will reach level two success for the project. The second test is to verify the custom ECU and ESB can run the engine safely in its stock configuration. The custom electronics are essential to collect data and to control the fuel flow into the engine. The custom ECU (Engine Control Unit) is shown as the green rectangular board on the left and the ESB (Engine Sensor Board) is the green curved board on the right. The third test is to integrate the REAPER recuperating design onto the engine and determine if the modified engine can run. Notice that the stock engine was exchanged with REAPER's modified engine components and the finned heat exchanger nozzle. The test setup is shown in Fig. 10.

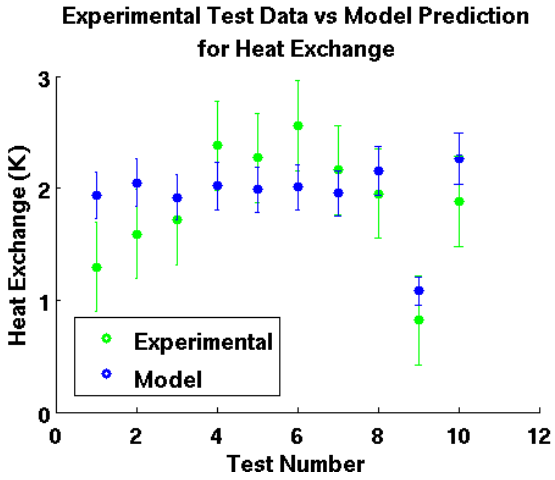

Figure 9. Experimental Test Data vs Model Prediction for Heat Exchange.

The final full system test is to determine if REAPER is able to improve the stock engine. This will be determined by collecting fuel flow and thrust data on the modified engine and comparing to stock engine results. With this test REAPER will compare test results to the model for level 3 success. If the results do not match REAPER will insert three additional thermocouples into the cold flow of the engine to trouble shoot and better understand the nature of the flow.

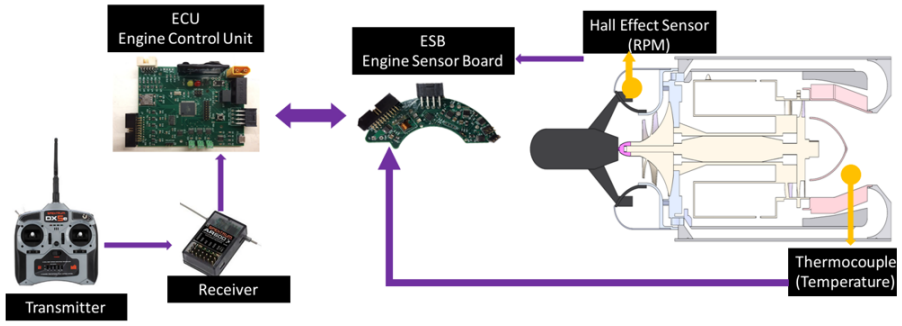

Figure 10. System Test with REAPER Recuperating Engine and REAPER Electronics.

V. Conclusion

To reach full project success the modified JetCat P90-RXi mini turbojet engine needed to decrease the thrust specific fuel consumption while maintaining all of the benefits of turbojet propulsion. In order to achieve that, two subsystems, engine electronics and internal engine airflow, were altered. The engine electronics included the Engine Control Unit (ECU) and Engine Sensor Board (ESB) and were custom built to provide the desired control over the engine when in its modified state. The second subsystem was a complete redesign of the engine which included new casings, finned nozzle heat exchanger. This redesign completely rerouted the internal airflow to make recuperation possible and ultimately increase the engine efficiency. The preliminary testing results showed that our control volume model was accurate within +5% of the experimental data. This test achieved complete level one success for both the recuperator and simulation side. In order to reach level 2 success further testing will take place later in the spring semester. REAPER will fully integrate the recuperator system on to the engine with the custom ECU and ESB running and monitoring the modified engine as it goes through the full throttle range. The conclusion of testing REAPER hopes to see a decrease in the Thrust Specific Fuel Consumption of the JetCat P-90 RXi jet engine. This project and future results can be used as a first iteration of designing and testing a recuperation system in mini-turbo jet engines to make them more fuel efficient.

References

[1] "Turbine Data Sheet." *JetCat USA*. 7-14-2015.

[2] Kakaç, S., and Hongtan Liu, *Heat Exchangers: Selection, Rating, and Thermal Design*, Boca Raton, FL: CRC, 1998. Print.

[3] Chi, S. W. Heat Pipe Theory and Practice: A Sourcebook. Washington, D.C.: Hemisphere Pub., 1976. Print.

[4] Zeigarnik, Yury A. "LIQUID-METAL HEAT TRANSFER." A-to-Z Guide to Thermodynamics, Heat & Mass Transfer, and Fluids Engineering. Thermopedia, 11 Feb. 2011. Web. 25 Sept. 2015.

[5] Contreras-Garcia, Julia, Emily Ehrle, Eric James, Jonathan Lumpkin, Matthew McClain, Megan O'Sullivan, Ben Woeste, and Kevin Wong, "COMET Project Final Report", 2014.

[6] Ma, Huikang, Daniel Frazier, Crawford Leeds, Corey Wilson, Carlos Torres, Alexander Truskowski, Christopher Jirucha, Abram Jorgenson, and Nathan Genrich, "MEDUSA Project Final Report", 2015. 09 Sept. 2015.

[7] Kuppan, T., *Heat Exchanger Design Handbook*, New York: CRC, 2013. Print.

[8] Kakaç, S., and Hongtan Liu, *Heat Exchangers: Selection, Rating, and Thermal Design*, Boca Raton, FL: CRC, 1998. Print.

[9] Moran, M.J., Shapiro, H.N., Munson, B.R., DeWitt, D.P, *Introduction to Thermal Systems Engineering: Thermodynamics, Fluid Mechanics, and Heat Transfer*, 1st ed., Wiley, New York, 2003.

[10] "Heat Exchangers", *Sondex Tapiro Oy Ab*, Web. 26 Sept. 2015.
<http://www.sondextapiro.fi/tuotteet/lammonsiirtimet_e.html>

[11] Wilson, D.G. and Korakianitis, T., *The Design of High-Efficiency Turbomachinery and Gas Turbines*, 2nd ed., The MIT Press, Cambridge, MA, 2003.

[12] Kays, W.M. and London, A.L., "Heat Exchanger Thermal and Pressure-Drop Design", *Compact Heat Exchanger Design*, R.R. Donnelley & Sons, 1984.

[13] "Stainless Steel - Grade 304", *Azo Materials*, Web. 11 Dec. 2015.
<http://www.azom.com/article.aspx?ArticleID=965>

[14] Lemmon, Eric W., Richard T. Thermodynamic Properties of Air and Mixtures of Nitrogen, Argon, and Oxygen From 60 to 2000 K at Pressure to 2000 MPa."Jacobsen, Steven G. Penocello, and Daniel G. Friend. "Journal of Physical Chemistry 29.3 (2000): 331-56. National Technical Reference Database. Web. 30 Nov. 2015. ¡http://www.nist.gov/data/PDFfiles/jpcrd581.pdf¿.

[15] Kadoya, K., M. Matsunaga, and A. Nagashima. "Viscosity and Thermal Conductivity of Dry Air in the Gaseous Phase." Journal of Physical Chemistry 14.4 (1985): 947-56. National Technical Reference Database. Web. 30 Nov. 2015. ¡http://www.nist.gov/data/PDFfiles/jpcrd283.pdf¿.

[16] Anderson, John D. *Computational Fluid Dynamics: The Basics with Applications*. 1st ed. New York: McGraw-Hill, 1995.

[17] SolidWorks Flow Simulation 2015. Dassault Systemes. 2015.

[18] "Flow Simulation 2015 Technical Manual," SolidWorks Flow Simulation 2105. Dassault Systemes. 2015.

[19] Cverna, Fran. *ASM Ready Reference. Thermal Properties of Metals*. Materials Park, Ohio: ASM International, 2002. Print.

[20] Vick, M.,"High Efficiency Recuperated Ceramic Gas Turbine Engines for Small Unmanned Air Vehicle Propulsion",Thesis, Imperial College of London, 31 Jan. 2012.

[21] McDonald, Colin F., Rodgers, Colin,"Small recuperated ceramic microturbine demonstrator concept", *Applied Thermal Engineering*, Volume 28, Issue 1, January 2008, Pages 60-74, ISSN 1359-4311. <http://dx.doi.org/10.1016/j.applthermaleng.2007.01.020>

[22] ”Capstone C200 Microturbine Technical Reference”, Capstone Turbine Corporation, June 2009. <http://www.regattasp.com/files/410066C_C200_Tech_Ref.pdf>

[23] Moran, M.J., Shapiro, H.N., Munson, B.R., DeWitt, D.P, *Introduction to Thermal Systems Engineering: Thermodynamics, Fluid Mechanics, and Heat Transfer*, 1st ed., Wiley, New York, 2003.

[24] ”JetCat RX Turbines with V10 ECU.” *JetCat Germany.* 2012.

[25] ”HAL 401: Linear Hall Effect Sensor IC.” *Micronas.* December 8, 2008.

[26] ”Disposable PFA Turnbin Flow Meter.” *Equflow Sensors.* February 2014.

[27] Miller, D.S., *Internal Flow Systems*, 2nd ed., BHRA Information Services, Cranfield, UK, 1990.